

THE IMPACT OF DAMPING COEFFICIENTS ON DYNAMIC BLADE MOTION OF FLEXIBLE SUBMERGED VEGETATION

Inga Prüter, TU Braunschweig, GERMANY, inga.prueter@tu-braunschweig.de

Kara Keimer, TU Braunschweig, GERMANY, k.keimer@tu-braunschweig.de

Felix Spröer, TU Braunschweig, GERMANY, felix.sproeer@tu-braunschweig.de

Oliver Lojek, TU Braunschweig, GERMANY, o.lojek@tu-braunschweig.de

Christian Windt, TU Braunschweig, GERMANY, c.windt@tu-braunschweig.de

Ioan Nistor, Dept. of Civil Engineering, University of Ottawa, CANADA, inistor@uottawa.ca

Nils Goseberg, TU Braunschweig, GERMANY, n.goseberg@tu-braunschweig.de

INTRODUCTION

Aquatic vegetation is known to provide several coastal ecosystem benefits, such as wave attenuation, sediment accumulation and soil stabilization (Rupprecht et al. 2017). To assess and quantify these benefits in the context of non-linear interactions between flexible submerged vegetation and hydrodynamic forces requires the advancement of state-of-the-art numerical models. An accurate estimation of the ecosystem benefits entails the consideration of field data, as a basis for an accurate modeling of the natural conditions in laboratory or numerical settings (e.g., Keimer et al. 2023). Empirically-derived parameters, such as the drag coefficient, are difficult to obtain from field data, requiring the employment of a numerical model that enables a direct coupling of the forces exerted by the hydrodynamic velocity and pressure field onto the vegetation elements. The open-source numerical model REEF3D::CFD has been used before in a one-way coupling of the forces by Martin and Bihs (2021). A two-way coupling that extends the previous work on aquaculture fish cage gear is now validated within the REEF3D::CFD frame work, aiming at an increased accuracy of the available numerical code.

OBJECTIVES AND NOVELTY

Aside from our validation effort to obtain a model toolbox for further studies, this work is the first study that attempts to investigate the influence of the damping coefficients (c_k) of the structural solver in REEF3D::CFD. The influence of c_k on the blade motion and the resulting forces under currents and waves is quantified, again, aiming to address the accuracy gap that current studies often show, when comparing against available experimental data.

METHODOLOGY

The fluid structure interaction (FSI) is simulated with the finite difference solver REEF3D::CFD, which features the level-set method used to define the free surface and high-order discretization schemes (Bihs et al. 2016). The fluid solver is based on the incompressible Navier-Stokes equations, coupled with a structural solver which is described by the geometrically exact Cosserat rod equations below:

$$\rho_s A \ddot{\underline{r}} = \frac{\partial \underline{f}}{\partial X} + \underline{f}_{ext} \quad (1)$$

$$\rho_s I \dot{\underline{\omega}} + \underline{\omega} \times \rho_s I \underline{\omega} = \frac{\partial \underline{m}}{\partial X} + \frac{\partial \underline{r}}{\partial X} \times \underline{f} + \underline{m}_{ext} \quad (2)$$

In Eqs. (1) and (2), ρ_s , A and I represent constant material parameters, i.e., the density of the solid, the area of the cross-section, and the second moments of inertia, respectively. While \underline{f} and \underline{m} describe the internal force and moment of the rod, respectively, \underline{f}_{ext} and \underline{m}_{ext} determine the external force and moment. Eq. (1) describes the translational motion $\underline{r}(X, t)$ by calculating the acceleration of the rod's centerline, for each Lagrangian coordinate $X \in [0; L]$. The rotational motion $R(X, t)$ of the rod is calculated by Eq. (2). The two-way coupling of the forces within the FSI model, visualized in Figure 1, is based on the implementation of Tschisgale and Fröhlich (2021).

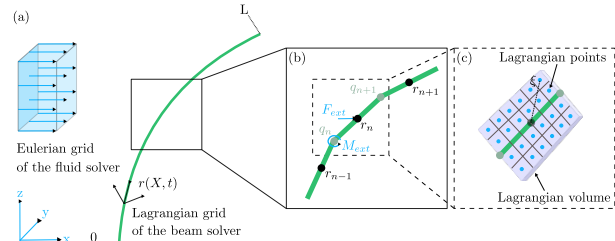


Figure 1 - (a) Definition sketch of the Cosserat rod and its coupling to the fluid solver with (b) applied forces and momentum for the rigid elements (c) as well as coupling of the Lagrangian points for an individual rigid element.

A convergence study (Cummins et al. 2017) has been carried out for both materials to be able to determine the necessary grid resolution to reproduce the forces acting on the blade. The resulting forces are compared for the refined cell size in the area around the blade for 0.75, 1.50 and 3.00 mm. For the intermediate cell size (1.50 mm), an average value (including a safety factor of 1.25 and the standard error of the fit) of the two materials was calculated, resulting in a grid uncertainty of 2.39% for the short blade and 10.42% for the long blade. The convergence study reveals that a fine grid close to the blade is crucial for an accurate simulation of the resulting forces. A non-uniform grid enables the use of a fine resolution of 1.5 mm in all three dimensions in the near-field of the blade.

In REEF3D::CFD, the time step size is calculated based on the CFL-criterion, which is used as an indicator of numerical convergence in the time domain. The CFL-criterion is only applied for the fluid solver and, hence, does not take the motion of the blade into account. Resulting forces for varying CFL-criterions (0.2 to 1.0) have been compared, with results differing by less than 0.0003 N. Therefore, the CFL-criterion was set equal to

1.0, which ensures a shorter simulation duration. Turbulence was simulated with a Large Eddy Simulation and a Smagorinsky subgrid-scale model. The structural solver was validated against physical experiments for two different types of material and hydrodynamic forces, such as current (Luhar and Nepf, 2011) and wave (Luhar and Nepf, 2016) conditions. In addition, different values of damping coefficients were tested and compared.

RESULTS

The validation results showed that the structural solver in REEF3D::CFD accurately simulates the FSI for all tested blade lengths, current velocities, waves, and material types. For the current simulations, the deviation of the tip position relative to the blade length was less than 10% (see Figure 2) for all blade lengths and material types and most simulated forces showed less than 10% deviation from the experimental forces.

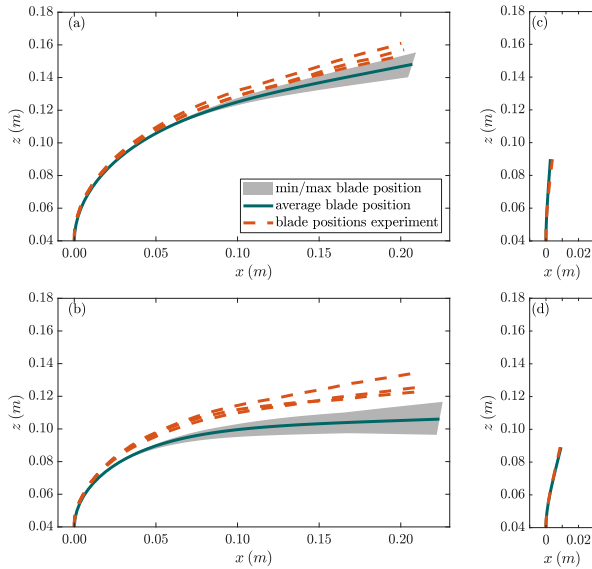


Figure 2 - Bending of the simulated and experimental blade with (a) and (b) $L_b = 0.25$ m, (c) and (d) $L_b = 0.05$ m and (a) and (c) $v = 0.16$ m/s and (b) and (d) $v = 0.32$ m/s

Furthermore, it was shown that the damping coefficient c_k determines the temporal response of the blade. Therefore, c_k does not affect the average forces calculated for the current simulations but impacts the movement of the blade position to a major extent. This behavior is important when the flow through a vegetation patch is considered in combination with sediment transport dynamics, where the feedback of the vegetation-influenced flow field is crucial to the sediment mobility solution. A variation of the drag force, as an indicator for the blade movement, is depicted in Figure 3 in the time and the frequency domain for different values of c_k . These results reveal that the highest c_k leads to fluctuations of the blade motion at a lower frequency compared to the other two values of c_k . Moreover, defining suitable damping coefficients is crucial for simulating the bending behavior and drag forces for flexible submerged vegetation under wave motion.

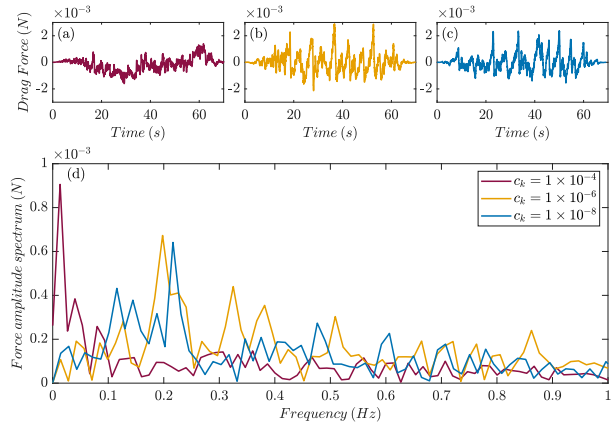


Figure 3 - (a) - (c) Simulated drag force in the time domain for different damping coefficients (c_k) and (d) force amplitude spectrum in the frequency domain.

CONCLUSIONS

Overall, the structural solver in REEF3D::CFD provides a powerful tool for simulating the FSI for flexible submerged vegetation. Future investigations are required to evaluate the relationship between the damping coefficients and material properties. Afterward, the implementation of field data will enable further conclusions regarding the coastal ecosystem benefits of flexible submerged vegetation.

REFERENCES

- Bihs, H., Kamath, A., Alagan Chella, M., Aggarwal, A., Arntsen, Øivind. (2016): A new level set numerical wave tank with improved density interpolation for complex wave hydrodynamics. *Computers & Fluids*, vol. 140.
- Cummins, C., Viola, I.M., Mastropaolo, E., Nakayama, N. (2017): The effect of permeability on the flow past permeable disks at low Reynolds numbers. *Physics of Fluids*, vol. 29.
- Keimer, K., Kosmalla, V., Prüter, I., Lojek, O., Prinz, M., Schürenkamp, D., Freund, H., Goseberg, N. (2023): Proposing a novel classification of growth periods based on biomechanical properties and seasonal changes of *Spartina anglica*. *Front. Mar. Sci.*, vol. 10.
- Luhar, M., Nepf, H.M. (2011): Flow-induced reconfiguration of buoyant and flexible aquatic vegetation. *Limnology and Oceanography*, vol. 56.
- Luhar, M., Nepf, H.M. (2016): Wave-induced dynamics of flexible blades. *Journal of Fluids and Structures*, vol. 61.
- Martin, T., Bihs, H. (2021): A numerical solution for modelling mooring dynamics, including bending and shearing effects, using a geometrically exact beam model. *JMSE*, vol. 9.
- Ruppel, F., Möller, I., Paul, M., Kudella, M., Spencer, T., Wesenbeeck, K., B., Wolters, G., Jensen, K., Bouma, T.J., Miranda-Lange, M., Schimmels, S. (2017): Vegetation-wave interactions in salt marshes under storm surge conditions. *Ecol. Eng.*, vol. 100.
- Tschisgale, S., Fröhlich, J. (2020): An immersed boundary method for the fluid-structure interaction of slender flexible structures in viscous fluid. *Journal of Computational Physics*, vol. 423.